

Communications to the Editor

N-Arylpiperazinone Inhibitors of Farnesyltransferase: Discovery and Biological Activity

Theresa M. Williams,* Jeffrey M. Bergman, Karen Brashear, Michael J. Breslin, Christopher J. Dinsmore, John H. Hutchinson, Suzanne C. MacTough, Craig A. Stump, Donna D. Wei, C. Blair Zartman, Michael J. Bogusky, J. Christopher Culberson, Carolyn Buser-Doepner,[†] Joseph Davide,[†] Ian B. Greenberg,[†] Kelly A. Hamilton,[†] Kenneth S. Koblan,[†] Nancy E. Kohl,[†] Dongming Liu,[†] Robert B. Lobell,[†] Scott D. Mosser,[†] Timothy J. O'Neill,[†] Elaine Rands,[†] Michael D. Schaber,[†] Francine Wilson,[†] Edith Senderak,[∇] Sherri L. Motzel,[‡] Jackson B. Gibbs,[†] Samuel L. Graham, David C. Heimbrook,[†] George D. Hartman, Allen I. Oliff,^{†,§} and Joel R. Huff

Departments of Medicinal Chemistry, Cancer Research, Molecular Systems, Laboratory Animal Resources, and Biometrics Research, Merck Research Laboratories, West Point, Pennsylvania 19486

Received May 24, 1999

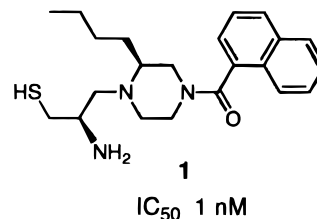
Introduction. Ras is a small GTP-binding protein intimately involved in cell signaling pathways and cell growth. Mutations arising in the Ras protein that impair GTP hydrolysis can lead to unregulated cell growth and cellular transformation. A mutated *ras* gene (*ras* oncogene) is often found in human tumors and is estimated to occur in 30–50% of colon and 90% of pancreatic cancers.¹

In 1989, it was discovered that farnesylation of a cysteine residue near the protein's C-terminus was required for its biological activity.² Interfering with Ras function by blocking the enzyme responsible for its farnesylation thus became a pharmacological target to suppress *ras*-dependent tumor growth. Since then, the efficacy of farnesyltransferase inhibitors (FTIs) in murine models of cancer has been demonstrated by their ability to inhibit H-, K-, and N-*ras*-dependent tumor growth in nude mice³ and induce tumor regression in H- and N-*ras* transgenic mice.⁴

FTIs have been obtained from a variety of sources, including natural product, proprietary sample collection, and combinatorial library screening, as well as rational design based upon the structure of farnesyl protein transferase (FTase) substrates.^{2,5} The C-terminal tetrapeptide of the Ras substrate constitutes a "Ca₁a₂X" box, a characteristic signal sequence for prenylation that

includes the reactive cysteine thiol. The a₁a₂ dipeptide adjacent to the prenylated cysteine residue is usually aliphatic and hydrophobic in nature, and in Ras proteins, X is either serine or methionine. Analogues of the Ca₁a₂X motif modified in a variety of ways are very efficient inhibitors of FTase in vitro.

FTIs based on the Ca₁a₂X tetrapeptide generally require the thiol and carboxylic acid functional groups of the natural protein FTase substrates for high enzyme affinity. However, it was desirable to re-engineer the peptide FTIs to achieve high levels of inhibition in the absence of these groups. Studies in vivo show that the highly polar carboxylic acid impedes cell penetration,⁶ while a thiol-containing drug has potential antigenic properties. An important consideration in the FTI drug design process was the overall minimization of peptide character, to maximize the chance of obtaining a drug with suitable pharmacokinetic properties. An earlier report describes our first attempt in this area, wherein truncation and conformational constraint of Ca₁a₂X peptides gave low-molecular-weight inhibitors such as **1**.⁷ These compounds maintained high levels of FTase inhibition in vitro (IC₅₀ 1 nM) and in vivo in the absence of the carboxylate.



Additional studies of Ca₁a₂X-based inhibitors indicate that imidazole is a very good cysteine surrogate, perhaps by serving as an alternative ligand for the FTase active site zinc ion.⁸ In an important discovery, attaching a benzyl group to the imidazole significantly improves potency relative to the unsubstituted imidazole.⁹ It seems likely that the added phenyl group takes advantage of a novel, high-affinity aryl-binding site, originally discovered in a separate investigation of Ca₁a₂X cysteine replacements.¹⁰ Potency on the order of the original Ca₁a₂X analogues was achieved with a variety of substituted benzylimidazole cysteine surrogates.⁹

In contrast to the Ca₁a₂X series, imidazole by itself is not a good cysteine surrogate in compounds such as **1**. The imidazole analogue **2a** experiences a 7000-fold loss in potency relative to aminothiols. Fortunately, however, the addition of a benzyl substituent to the imidazole ring boosts potency 10-fold in the 1,5-isomer **2a** (IC₅₀ 495 nM). As previously observed in the tetrapeptide series, this effect is highly dependent on the regiochemistry of imidazole alkylation (e.g. the 1,4-substituted imidazole isomer of **2a** has an IC₅₀ > 100 000 nM). Substituents on the benzyl ring that

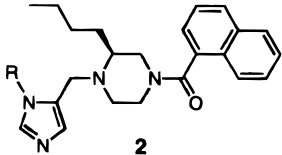
* Department of Cancer Research.

† Department of Molecular Systems.

∇ Department of Biometrics Research.

‡ Department of Laboratory Animal Resources.

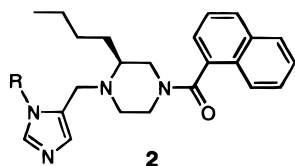
§ Current address: DuPont Pharmaceuticals Co., Rte 141 and Henry Clay Rd, Wilmington, DE 19880.

Table 1. Influence of Imidazole Substitution on Activity


entry	R	FTase IC ₅₀ (nM) ^a	
2a	H	7300 ± 2100	(n = 2)
2b	PhCH ₂	495 ± 65	(n = 2)
2c	(4-CN)PhCH ₂	21 ± 1	(n = 2)

^a Concentration of compound required to inhibit 50% of FTase-catalyzed incorporation of [³H]FPP into recombinant human K-Ras protein. Assay results were obtained using the protocol described in ref 6.

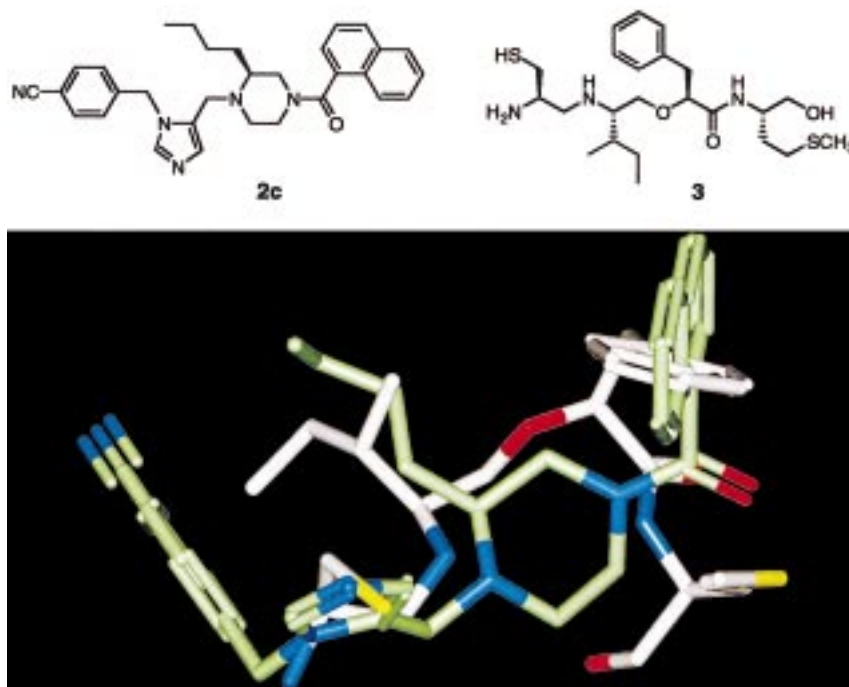
enhanced potency in the Ca₁a₂X series were also screened in the present context. The most dramatic increase in activity relative to **2a** results from introducing a *p*-cyano group, giving benzylimidazole analogue **2c** (IC₅₀ 21 nM) (Table 1). Other substitutions on the benzyl ring are less effective or detrimental to activity, suggesting an as-yet unknown specific interaction for the cyano group.



A computer-generated overlay using both electrostatic and steric parameters¹¹ matches conformations of **2c** with the conformation of FTase-bound CIFM analogue **3**.¹² The best-fit superpositions have the putative zinc ligand imidazole of **2c** overlaid with the aminothiols in **3**, the *N*-aryl substituent of **2c** positioned near the hydrophobic a₂ substituent of **3**, and the *n*-butyl group

aligned with the a₁ substituent of **3** (Figure 1). In this model, the acyl group in **2c** occupies a region of space similar to the lone amide carbonyl group necessary for potency in Ca₁a₂X analogues. In the overlay, the cyanobenzyl substituent in **2c** did not correlate to any part of **3**. From inspection of models, it is evident that a slight rearrangement of functional groups to give *N*-arylpiperazinone **4a** similarly overlays the enzyme-bound conformation of **3** (Figure 2). On the basis of this observation, piperazinone **4a** was synthesized and subsequently determined to be our first subnanomolar FTI without thiol or carboxylic acid functional groups. We are currently establishing structure–activity relationships (SAR) within this series, with respect to both intrinsic FTase potency and ability to block proliferation of *ras*-transformed cells, and wish to report our preliminary results.

Chemistry. The synthesis of **4a** proceeds as described in Scheme 1 and is illustrative of the general procedure. The Weinreb amide of *N*-Boc-*L*-norleucine is reduced to the aldehyde, which undergoes reductive alkylation with 2,3-dimethylaniline in the presence of sodium triacetoxyborohydride to produce *N*-arylated ethylenediamine **6**. Chloroacetylation followed by base-induced cyclization furnishes the protected piperazinone **8**. The regioselective alkylation of 4-hydroxymethylimidazole utilizes chemistry developed by Anthony et al. for the synthesis of regiochemically defined substituted imidazoleacetic acid esters.⁹ Thus, the less hindered nitrogen of 4-hydroxymethylimidazole reacts with trityl chloride to give exclusively the trityl-protected 1,4-substituted isomer. Fully protected trityl acetate **9** is alkylated with 4-cyanobenzyl bromide to form the imidazolium salt, which undergoes solvolysis in refluxing methanol to imidazole hydrobromide **10**. Acetate hydrolysis and oxidation produces aldehyde **12**, which

**Figure 1.** Computer-generated overlay of piperazine **2c** and CIFM analogue **3**.

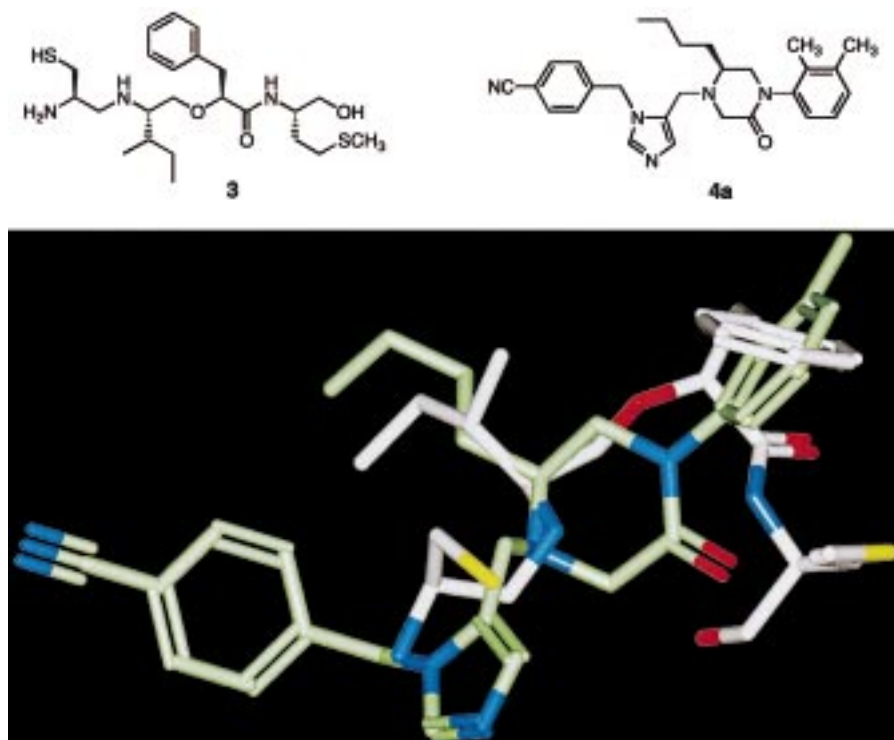
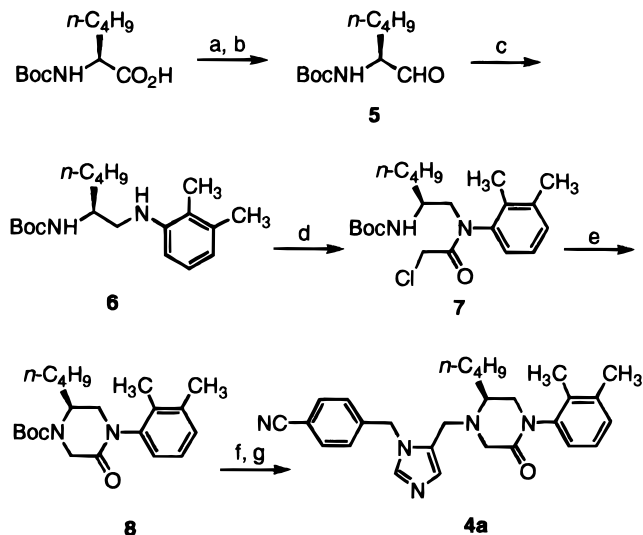


Figure 2. Computer-generated overlay of CIFM analogue **3** and piperazinone **4a**.

Scheme 1. General Synthesis of Piperazinone FTIs^a

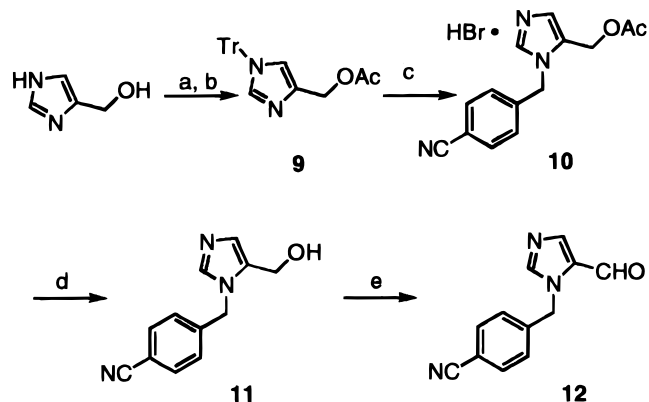


^a (a) $\text{CH}_3\text{NHOCH}_3$, EDC, HOBT, $(\text{C}_2\text{H}_5)_3\text{N}$, DMF, 95%; (b) LiAlH_4 , $(\text{C}_2\text{H}_5)_2$, $45-0^\circ\text{C}$, 100%; (c) ArNH_2 , $\text{NaBH}(\text{OAc})_3$, DCE, pH 6, 20°C , 63%; (d) ClCH_2COCl , aq NaHCO_3 , $\text{CH}_3\text{CO}_2\text{C}_2\text{H}_5$, 0°C ; (e) Cs_2CO_3 , DMF, $0-20^\circ\text{C}$, 96%; (f) HCl , $\text{CH}_3\text{CO}_2\text{C}_2\text{H}_5$; (g) RCHO , $\text{NaBH}(\text{OAc})_3$, DCE, pH 6, 20°C , 61%.

is reductively alkylated with the deprotected form of piperazinone **8** to give the desired imidazole isomer **4a**.

Results and Discussion. The initial compound prepared in the piperazinone series, **4a**, inhibits FTase with an IC_{50} of 0.4 nM (Table 2). Structure-activity studies show that substitution of the *N*-aryl ring with hydrophobic groups in either the *ortho*- or *meta*-positions is well-tolerated. Small hydrophobic groups in the *meta*-position (**4b**, **4c**) in particular give highly potent inhibitors ($\text{IC}_{50} \leq 0.1$ nM). Variation of the piperazinone C-5 substituent demonstrates that the *S* stereochemistry is preferred over the *R* by a factor of 10 (compare

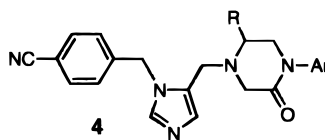
Scheme 2. Synthesis of Imidazole Intermediate^a



^a (a) Ph_3CCl , $(\text{C}_2\text{H}_5)_3\text{N}$, DMF, 20°C , 1 h, 94%; (b) $(\text{CH}_3\text{CO})_2\text{O}$, pyr, 20°C , 5 h, 97%; (c) i. ArCH_2Br , $\text{CH}_3\text{CO}_2\text{C}_2\text{H}_5$, 55°C , 24 h, ii. CH_3OH , 55°C ; (d) LiOH , THF, H_2O , 0°C , 1 h, 66%; (e) $\text{SO}_3\text{-pyr}$, $(\text{C}_2\text{H}_5)_3\text{N}$, DMSO, 20°C , 2 h, 80%.

4d, **4e**). Intrinsic FTase potency increases with the length of the C-5 alkyl group; a C-5 butyl or ethylsulfonylethylmethyl substituent (**4c**, **4f**) increases potency 20–100-fold relative to the methyl-substituted analogue **4d**. Consistent with the model aligning the C-5 substituent with the a_1 side chain in $\text{Ca}_{1.2}\text{X}$ analogues, the most active compounds contain hydrophobic groups at this position. Moderately polar substituents such as sulfones are also tolerated (**4f**).

To determine the ability of the compounds to act intracellularly, compounds were assayed for their ability to inhibit 50% of the anchorage-independent growth of cultured *H-ras*-transformed RAT1 cells on poly(HEMA)-coated microtiter plates (Table 3). In this assay, **4b** and **4f** have IC_{50} values between 1 and 10 nM. These concentrations are well below the $10\ \mu\text{M}$ to $>100\ \mu\text{M}$ concentrations that are compatible with survival of 80–90% of normal RAT1 cells, as determined by viable

Table 2. Influence of *N*-Aryl and Piperazinone Substitution on Activity

entry	Ar	R	FTase IC ₅₀ (nM) ^a		GGTase IC ₅₀ (nM) ^b	
4a	2,3-Me ₂ Ph	(<i>S</i>)- <i>n</i> -C ₄ H ₉	0.44 ± 0.5	(<i>n</i> = 2)	10000	(<i>n</i> = 1)
4b	3-CF ₃ OPh	(<i>S</i>)- <i>n</i> -C ₄ H ₉	<0.15 ± 0.07	(<i>n</i> = 3)	12000	(<i>n</i> = 1)
4c	3-ClPh	(<i>S</i>)- <i>n</i> -C ₄ H ₉	0.11 ± 0.02	(<i>n</i> = 3)	NT	
4d	3-ClPh	(<i>S</i>)-CH ₃	9 ± 1	(<i>n</i> = 2)	NT	
4e	3-ClPh	(<i>R</i>)-CH ₃	80 ± 0	(<i>n</i> = 2)	NT	
4f	3-ClPh	(<i>R</i>)-C ₂ H ₅ SO ₂ CH ₂ ^c	0.18 ± 0.11	(<i>n</i> = 3)	>100000	(<i>n</i> = 1)

^a Concentration of compound required to inhibit 50% of FTase-catalyzed incorporation of [³H]FPP into recombinant human K-Ras protein. Assay results were obtained using the protocol described in ref 6. ^b Concentration of compound required to inhibit 50% of GGTase I-catalyzed incorporation of [³H]GGPP into recombinant human RhoA protein. Assay results were obtained using the protocol described in ref 6. ^c Compound **4f** has the same absolute stereochemistry as compounds **4a–d**, but group priority rules lead to the “*R*” designation.

Table 3. Effect of Piperazinone FTIs on Cell Growth

entry	poly(HEMA) IC ₅₀ (nM) ^a			soft agar IC ₉₀ (nM) ^b			cytotoxic endpoint IC ₂₀ (μM) ^c
	H- <i>ras</i>	MCF7	DLD1	H- <i>ras</i>	K- <i>ras</i>		
4a	28 ± 16 (<i>n</i> = 4)	NT ^d	NT	100–1000 ^e (<i>n</i> = 2)	2500–10000 (<i>n</i> = 2)	25–50 (<i>n</i> = 4)	
4b	2 ± 1 (<i>n</i> = 28)	4 ± 1 (<i>n</i> = 2)	660 ± 8 (<i>n</i> = 2)	3–30 (<i>n</i> = 2)	30–100 (<i>n</i> = 2)	15 (<i>n</i> = 5)	
4f	8 ± 4 (<i>n</i> = 9)	5 ± 1 (<i>n</i> = 2)	1500 ± 200 (<i>n</i> = 2)	30 (<i>n</i> = 1) ^f	1000 (<i>n</i> = 2)	>100 (<i>n</i> = 1)	

^a Concentration of compound required to inhibit 50% of cell growth on poly(HEMA)-coated microtiter plates. The assay is based on conditions reported in ref 19 and is a measure of anchorage-independent cell growth. ^b The concentration of compound required to inhibit the anchorage-independent growth by 90% of either human H- or K-*ras*-transformed RAT1 cells suspended in soft agar, as compared to vehicle-treated control. Assay conditions are described in ref 20. ^c Highest concentration of compound compatible with 80% cell survival in cultured RAT1 cells, as assessed by viable staining with MTT. Assay conditions are described in ref 21. ^d Not tested. ^e Determined in viral H-*ras*-transformed RAT1 cells. ^f A second determination in viral H-*ras*-transformed RAT1 cells gave an identical result.

staining. To account for the differential effect of FTIs on normal versus tumor tissue, there is evidence that FTIs can induce apoptosis selectively in transformed cells under certain conditions.¹³

In another measure of anchorage-independent growth inhibition, compounds **4a**, **4b**, and **4f** were assayed for their ability to block colony formation of H- and K-*ras*-transformed RAT1 cells suspended in soft agar. One of the most active compounds in this assay, **4b**, inhibits 90% of H-Ras colony formation (IC₉₀) at concentrations between 3 and 30 nM, well below the 10 000 nM concentration that elicits 10–20% cytotoxicity in normal RAT1 cells (Table 3). While H-Ras is an exclusive substrate for FTase, one complicating feature of Ras biology relates to the ability of K-Ras to be a substrate for either FTase or GGTase I.¹⁴ Since both prenylated forms of the protein are capable of transforming cells, it is reasonable to assume that both FTase and GGTase I need to be suppressed to observe optimal effects on K-*ras*-mediated cell growth.¹⁵ Although compounds **4a**, **4b**, and **4f** are poor inhibitors of GGTase I (IC₅₀ values greater than 10 000 nM, Table 2), they block 90% of colony formation in K-*ras*-transformed RAT1 cell lines at concentrations not toxic to normal RAT1 cells (Table 3). Compared to cells expressing H-Ras, however, approximately 10–30-fold higher concentrations of these compounds are needed to inhibit K-*ras*-transformed cell proliferation to the same extent. For example, FTI **4b** blocks K-Ras colony formation with an IC₉₀ of 30–100 nM, a 3–10-fold increase relative to its IC₉₀ in H-*ras*-transformed cells. Overall, it is not well-understood why selective FTIs interfere with proliferation of K-*ras*-transformed cells. One possibility is

Table 4. Selective FTIs Inhibit Both H-*ras* and K-*ras* Tumor Growth in Nude Mice^a

entry	cell line	dose	tumor growth inhibition (%)
4b	H- <i>ras</i> /Rat1	40 ^b	100 (<i>P</i> < 0.01) ^d
4b	H- <i>ras</i> /Rat1	10 ^b	68 (<i>P</i> < 0.01)
4b	K- <i>ras</i> /Rat1	80 ^b	64 (<i>P</i> < 0.05)
4f	H- <i>ras</i> /Rat1	14 ^c	100 (<i>P</i> < 0.01)
4f	H- <i>ras</i> /Rat1	1.4 ^c	73 (<i>P</i> < 0.01)
4f	K- <i>ras</i> /Rat1	14 ^c	60 (<i>P</i> < 0.01)

^a Female nude mice were subcutaneously injected with either H- or K-*ras*-transformed RAT1 cells. After 24 h animals were treated with either vehicle or FTI (*n* = 8–10). Compound was administered either by subcutaneous injection or by surgically implanted Alzet osmotic pumps delivering 5 mL/h vehicle (50% DMSO/water) or compound over a period of approximately 14 days. ^b Administered by subcutaneous injection. ^c Administered by continuous infusion. ^d Statistical significance of tumor growth inhibition, relative to vehicle-treated control mice.

that other (non-Ras) farnesylated proteins are responsible for the observed effects on growth in transformed cells.¹⁶

In vivo studies in mice corroborate the activity observed in cell culture.¹⁷ In nude mice bearing either H- or K-*ras*-dependent tumors, treatment with **4b** or **4f** for approximately 2 weeks produces statistically significant tumor growth inhibition relative to vehicle-treated controls. Compounds are administered either subcutaneously once per day (**4b**) or by continuous subcutaneous (sc) infusion via implanted Alzet minipump (**4f**). In mice implanted with H-*ras*-transformed cells, 100% of tumor growth is blocked with either 40 mg/kg/day **4b** or 14 mg/kg/day **4f** (Table 4). Approximately 8–10-fold higher doses are required to block the same degree of K-*ras* tumor growth compared to H-*ras*. A 68% reduction in tumor size occurs upon treatment of H-*ras*

tumors with 10 mg/kg/day **4b**, but 80 mg/kg/day **4b** is required to produce a 64% reduction in *K-ras* tumors. Similarly for **4f**, 1.4 mg/kg/day gives 73% reduction in *H-ras* tumors, but 14 mg/kg/day is needed for 60% inhibition of *K-ras* tumor growth.

Human tumor cell lines exhibit varying degrees of sensitivity to FTIs **4b** and **4f**. In the MCF7 cell line, **4b** and **4f** have IC₅₀ values of 4 and 5 nM, respectively, in the monolayer anchorage-independent growth assay (Table 3). With the DLD1 cell line, **4b** and **4f** have IC₅₀ values of 660 and 1500 nM, respectively. As noted in earlier reports, the growth-inhibiting effect of FTIs on cultured human tumor cell lines is largely independent of their *ras* mutational status,¹⁸ and one of the most sensitive cell lines, MCF7, is known to possess the wild-type *ras*. It is possible that this and similar cell lines contain activating mutations in proteins that function upstream of Ras in the MAP/K signal transduction pathway.

Conclusion. Beginning with inhibitors that were derived from the FTase Ras substrate Ca₁a₂X tetrapeptide, a series of modifications led to non-thiol, non-carboxylate piperazinone FTIs that achieve potent levels of inhibition. Significant aspects of inhibitor design en route to **2c** include conformational constraint via a piperazine ring, optimization of the piperazine *N*-acyl hydrophobic substituent, replacement of cysteine with imidazole, and optimization of the imidazole substituent to take advantage of a new high-affinity FTase binding site. Modeling studies based on the FTase-bound conformation of a tetrapeptide analogue provided the inspiration to pursue piperazinone **4a** and analogues. These compounds are subnanomolar FTIs that potentially inhibit the anchorage-independent growth of both *H*- and *K-ras*-transformed cells and inhibit tumor growth in a mouse tumor model. The overall profile of piperazinone FTIs, including their ability to suppress the anchorage-independent growth of human tumor cell lines at reasonable concentrations, encourages us to continue to optimize their properties in the hope of obtaining a clinically useful anticancer agent.

Acknowledgment. The authors would like to thank Graham M. Smith, Kenneth D. Anderson, Patrice A. Ciecko, and Matthew M. Zrada for elemental analyses and Harri J. Ramjit, Arthur B. Coddington, and Charles W. Ross for mass spectra for the reported compounds. We are also indebted to A. Burkhardt, D. Chen, Ronald E. Diehl, Astrid M. Kral, Charles A. Omer, and Patricia J. Miller for their assistance in carrying out mouse experiments. Finally, we are grateful to Joy M. Hartzell for preparation of this manuscript.

References

- Rodenhuis, S. Ras and Human Tumors. *Semin. Cancer Biol.* **1992**, *3*, 241–247.
- Leonard, D. M. Ras Farnesyltransferase: A New Therapeutic Target. *J. Med. Chem.* **1997**, *40*, 2971–2990.
- Kohl, N. E.; Wilson, F. R.; Mosser, S. D.; Giuliani, E. A.; deSolms, S. J.; Conner, M. W.; Anthony, N. J.; Holtz, W. J.; Gomez, R. P.; Lee, T.-J.; Smith, R. L.; Graham, S. L.; Hartman, G. D.; Gibbs, J. B.; Oliff, A. Protein Farnesyltransferase Inhibitors Block the Growth of *ras*-Dependent Tumors in Nude Mice. *Proc. Natl. Acad. Sci. U.S.A.* **1994**, *91*, 9141–9145.
- (a) Kohl, N. E.; Omer, C. A.; Conner, M. W.; Anthony, N. J.; Davide, J. P.; deSolms, S. J.; Giuliani, E. A.; Gomez, R. P.; Graham, S. L.; Hamilton, K.; Handt, L. K.; Hartman, G. D.; Koblan, K. S.; Kral, A. M.; Miller, P. J.; Mosser, S. D.; O'Neill, T. J.; Shaber, M. D.; Gibbs, J. B.; Oliff, A. Inhibition of Farnesyltransferase Induces Regression of Mammary and Salivary Carcinomas in *ras* Transgenic Mice. *Nature Medicine* **1995**, *1*, 792–797. (b) Manguerra, R.; Corral, T.; Kohl, N. E.; Symmans, W. F.; Lu, S.; Malumbres, M.; Gibbs, J. B.; Oliff, A.; Pellicer, A. Antitumor Effect of a Farnesyl Protein Transferase Inhibitor in Mammary and Lymphoid Tumors Overexpressing *N-ras* in Transgenic Mice. *Cancer Res.* **1998**, *58*, 1253–1259.
- Williams, T. M.; Dinsmore, C. J. Farnesyl Transferase Inhibitors: Design of a New Class of Cancer Chemotherapeutic Agents. In *Advances in Medicinal Chemistry*; Maryanoff, B. E., Reitz, A. B., Eds.; JAI Press: Greenwich, CT, 1999; Vol. 4; pp 273–314.
- Graham, S. L.; deSolms, S. J.; Giuliani, E. A.; Kohl, N. E.; Mosser, S. D.; Oliff, A. I.; Pompliano, D. L.; Rands, E.; Breslin, M. J.; Deana, A. A.; Garsky, V. M.; Scholz, T. H.; Gibbs, J. B.; Smith, R. L. Pseudopeptide Inhibitors of Ras Farnesyl-Protein Transferase. *J. Med. Chem.* **1994**, *37*, 725–732.
- Williams, T. M.; Ciccarone, T. M.; MacTough, S. C.; Bock, R. L.; Conner, M. W.; Davide, J. P.; Hamilton, K.; Koblan, K. S.; Kohl, N. E.; Kral, A. M.; Mosser, S. D.; Omer, C. A.; Pompliano, D. L.; Rands, E.; Schaber, M. D.; Shah, D.; Wilson, F. R.; Gibbs, J. B.; Graham, S. L.; Hartman, G. D.; Oliff, A. I.; Smith, R. L. 2-Substituted Piperazines as Constrained Amino Acids. Application to the Synthesis of Potent, Non Carboxylic Acid Inhibitors of Farnesyltransferase. *J. Med. Chem.* **1996**, *39*, 1345–1348.
- (a) Hunt, J. T.; Lee, V. G.; Leftheris, K.; Seizinger, B.; Carboni, J.; Mabus, J.; Ricca, C.; Yan, N.; Manne, V. Potent, Cell Active, Non-Thiol Tetrapeptide Inhibitors of Farnesyltransferase. *J. Med. Chem.* **1996**, *39*, 353–358. (b) Park, H.-W.; Boduluri, S. R.; Moomaw, J. F.; Casey, P. J.; Beese, L. S. Crystal Structure of Protein Farnesyltransferase at 2.25 Angstrom Resolution. *Science* **1997**, *275*, 1800–1804. (c) Strickland, C. L.; Windsor, W. T.; Syto, R.; Wang, L.; Bond, R.; Wu, Z.; Schwartz, J.; Le, H. V.; Beese, L. S.; Weber, P. C. Crystal Structure of Farnesyl Protein Transferase Complexed with a CaaX Peptide and Farnesyl Diphosphate Analogue. *Biochemistry* **1998**, *37*, 16601–16611. (d) Hightower, K. E.; Huang, C. C.; Casey, P. J.; Fierke, C. A. H-Ras Peptide and Protein Substrates Bind Protein Farnesyltransferase as an Ionized Thiolate. *Biochemistry* **1998**, *37*, 15555–15562.
- Anthony, N. J.; Gomez, R. P.; Schaber, M. D.; Mosser, S. D.; Hamilton, K. A.; O'Neill, T. J.; Koblan, K. S.; Graham, S. L.; Hartman, G. D.; Shah, D.; Rands, E.; Kohl, N. E.; Gibbs, J. B.; Oliff, A. I. Design and In Vivo Analysis of Potent Nonthiol Inhibitors of Farnesyl Protein Transferase. *J. Med. Chem.* **1999**, *42*, 3356–3368.
- Breslin, M. J.; deSolms, S. J.; Giuliani, E. A.; Stokker, G. E.; Graham, S. L.; Pompliano, D. L.; Mosser, S. D.; Hamilton, K. A.; Hutchinson, J. H. Potent, Non-Thiol Inhibitors of Farnesyltransferase. *Bioorg. Med. Chem.* **1998**, *8*, 3311–3316.
- Miller, M.; Sheridan, R. P.; Kearsley, S. K. SQ, A Program for Rapidly Producing Pharmacophorically Relevant Molecular Superpositions. *J. Med. Chem.* **1999**, *42*, 1505–1514.
- Koblan, K. S.; Culbertson, J. C.; deSolms, S. J.; Giuliani, E. A.; Mosser, S. D.; Omer, C. A.; Pitznerberger, S. M.; Bogusky, M. J. NMR Studies of Novel Inhibitors Bound to Farnesyl-Protein Transferase. *Protein Sci.* **1995**, *4*, 681–688.
- (a) Lebowitz, P. F.; Sakamuro, D.; Prendergast, G. C. Farnesyl Transferase Inhibitors Induce Apoptosis of Ras-transformed Cells Denied Substratum Attachment. *Cancer Res.* **1997**, *57*, 708–713. (b) Suzuki, N.; Urano, J.; Tamanoi, F. Farnesyltransferase Inhibitors Induce Cytochrome C Release and Caspase 3 Activation Preferentially in Transformed Cells. *Proc. Natl. Acad. Sci. U.S.A.* **1998**, *95*, 15356–15361.
- (a) Trueblood, C. E.; Ohya, Y.; Rine, J. Genetic Evidence for in vivo Cross-Specificity of the CaaX-Box Protein Prenyltransferases Farnesyltransferase and Geranylgeranyltransferase-I in *Saccharomyces cerevisiae*. *Mol. Cell. Biol.* **1993**, *13*(7), 4260–4275. (b) Whyte, D. B.; Kirschmeier, P.; Hockenberry, T. N.; Nunez-Oliva, I.; James, L.; Catino, J. J.; Bishop, R. B.; Pai, J.-K. K- and N-Ras are Geranylgeranylated in Cells Treated with Farnesyl Protein Transferase Inhibitors. *J. Biol. Chem.* **1997**, *272*, 14459–14464. (c) Rowell, C. A.; Kowalczyk, J. J.; Lewis, M. D.; Garcia, A. M. Direct Demonstration of Geranylgeranylation and Farnesylation of K-Ras in Vivo. *J. Biol. Chem.* **1997**, *272*, 14093–14097.
- Lerner, E. C.; Zhang, T.-T.; Knowles, D. B.; Quiam, Y.; Hamilton, A. D.; Sebt, S. M. Inhibition of the Prenylation of K-Ras, But Not H- or N-Ras, is Highly Resistant to CAAX Peptidomimetics and Requires Both a Farnesyltransferase and a Geranylgeranyltransferase I Inhibitor in Human Tumor Cell Lines. *Oncogene* **1997**, *15*, 1283–1288.
- (a) Gibbs, J. B.; Graham, S. L.; Hartman, G. D.; Koblan, K. S.; Kohl, N. E.; Omer, C. A.; Oliff, A. Farnesyltransferase Inhibitors versus Ras Inhibitors. *Curr. Opin. Chem. Biol.* **1997**, *1*, 197–203. (b) Cox, A. D.; Der, C. J. Farnesyltransferase Inhibitors and

- Cancer Treatment: Targeting Simply Ras? *Biochim. Biophys. Acta* **1997**, *1333*, F51–F71. (c) Lebowitz, P. F.; Prendergast, G. C. Non-Ras Targets of Farnesyltransferase Inhibitors: Focus on Rho. *Oncogene* **1998**, *17*, 1439–1445.
- (17) Sun, J.; Quian, Y.; Hamilton, A. D.; Sebt, S. M. Both Farnesyltransferase and Geranylgeranyltransferase I Inhibitors are Required for Inhibition of Oncogenic K-Ras Prenylation But Each Alone is Sufficient to Suppress Human Tumor Growth in Nude Mouse Xenografts. *Oncogene* **1998**, *16*, 1467–1473.
- (18) Sepp-Lorenzino, L.; Ma, Z.; Rands, E.; Kohl, N.; Gibbs, J. B.; Oliff, A.; Rosen, N. A Peptidomimetic Inhibitor of Farnesyl: Protein Transferase Blocks the Anchorage-dependent and Independent Growth of Human Tumor Cell Lines. *Cancer Res.* **1995**, *55*, 5302–5309.
- (19) Fukazawa, H.; Nakano, S.; Mizuno, S.; Uehara, Y. Inhibitors of Anchorage-Independent Growth Affect the Growth of Transformed Cells on Poly(2-hydroxyethyl methacrylate)-Coated Surfaces. *Int. J. Cancer* **1996**, *67*, 876.
- (20) Kohl, N. E.; Mosser, S. D.; deSolms, S. J.; Giuliani, E. A.; Pompliano, D. L.; Graham, S. L.; Smith, R. L.; Scolnick, E. M.; Oliff, A. I.; Gibbs, J. B. Selective Inhibition of Ras-Dependent Transformation By A Farnesyltransferase Inhibitor. *Science* **1993**, *260*, 1934–1937.
- (21) Mossman, T. Rapid Colorimetric Assay for Cellular Growth and Survival: Application to Proliferation and Cytotoxicity Assays. *J. Immunol. Methods* **1983**, *65*, 55–63.

JM990254Z